Temporary loss of perivascular aquaporin-4 in neocortex after transient middle cerebral artery occlusion in mice

Didrik S. Frydenlund*, Anish Bhardwaj[†‡], Takashi Otsuka[†], Maria N. Mylonakou*, Thomas Yasumura[§], Kimberly G. V. Davidson[§], Emil Zeynalov[†], Øivind Skare[¶], Petter Laake[¶], Finn-Mogens Haug*, John E. Rash[§‖], Peter Agre**[††], Ole P. Ottersen*[††], and Mahmood Amiry-Moghaddam*[††]

*Nordic Centre of Excellence for Research in Water Imbalance Related Disorders (WIRED), Centre for Molecular Biology and Neuroscience, Department of Anatomy, University of Oslo, P.O. Box 1105, 0317 Oslo, Norway; [¶]Department of Biostatistics, Institute for Basic Medical Sciences, University of Oslo, 0317 Oslo, Norway; Departments of [†]Anesthesiology and Critical Care Medicine and [‡]Neurology, Johns Hopkins University School of Medicine, Baltimore, MD 21205; [§]Department of Biomedical Sciences and [‖]Program in Molecular, Cellular, and Integrative Neuroscience, Colorado State University, Fort Collins, CO 80523-1617; and **Duke University School of Medicine, Durham, NC 27710

Contributed by Peter Agre, July 11, 2006

The aquaporin-4 (AQP4) pool in the perivascular astrocyte membranes has been shown to be critically involved in the formation and dissolution of brain edema. Cerebral edema is a major cause of morbidity and mortality in stroke. It is therefore essential to know whether the perivascular pool of AQP4 is up- or down-regulated after an ischemic insult, because such changes would determine the time course of edema formation. Here we demonstrate by quantitative immunogold cytochemistry that the ischemic striatum and neocortex show distinct patterns of AQP4 expression in the reperfusion phase after 90 min of middle cerebral artery occlusion. The striatal core displays a loss of perivascular AQP4 at 24 hr of reperfusion with no sign of subsequent recovery. The most affected part of the cortex also exhibits loss of perivascular AQP4. This loss is of magnitude similar to that of the striatal core, but it shows a partial recovery toward 72 hr of reperfusion. By freeze fracture we show that the loss of perivascular AQP4 is associated with the disappearance of the square lattices of particles that normally are distinct features of the perivascular astrocyte membrane. The cortical border zone differs from the central part of the ischemic lesion by showing no loss of perivascular AQP4 at 24 hr of reperfusion but rather a slight increase. These data indicate that the size of the AQP4 pool that controls the exchange of fluid between brain and blood during edema formation and dissolution is subject to large and region-specific changes in the reperfusion phase.

astrocytes | brain edema | ischemia | stroke | water channels

Stroke is invariably associated with a brain edema that accounts for much of the morbidity and mortality of this condition. The brain edema is often long lasting and therapy-resistant and thus poses a major challenge in the clinic. A better understanding is needed of the molecular mechanisms that promote water flux across the brain–blood interface in the build-up phase and resolution phase of cerebral edema.

Aquaporin-4 (AQP4) water channels are strongly enriched in the astrocyte plasma membrane domains that ensheathe the cerebral microvessels (1, 2). It was hypothesized (1) that this perivascular pool of AQP4 could become rate-limiting for water flux in pathophysiological conditions, such as in the reperfusion phase after an ischemic insult. This hypothesis was tested in a model that took advantage of the fact that the perivascular AQP4 pool is anchored through the dystrophin complex (comprising the brain dystrophin isoform DP-71 and α-syntrophin) (3). Mice with targeted deletion of α-syntrophin displayed a dramatic loss of perivascular AQP4 and a concomitant reduction in the extent of postischemic edema (4). These findings [and experiments in mdx mice (5)] support the idea that the perivascular pool of AQP4 facilitates water flux across the brain–blood interface and offer a mechanistic explanation for the reduction in brain edema formation and dissolution observed in AQP4$^{-/-}$ animals (6, 7) The implication of a specialized class of membrane molecule in the pathophysiology of brain edema instills hope for new therapy that could complement the current treatment strategies based on surgical decompression or infusion of hyperosmolar solutions.

A critical question is whether the perivascular pool of AQP4 is down- or up-regulated during or after a transient ischemic insult. If astrocytes respond to ischemia by down-sizing the perivascular pool of AQP4, this would delimit water uptake but would also reduce the potential for any therapeutic intervention targeting AQP4.

The aim of this work was to unravel the time course of AQP4 expression at the blood–brain interface, after transient ischemia induced by middle cerebral artery occlusion (MCAO). The postembedding immunogold procedure is uniquely suited to this task, because it offers a semiquantitative assessment of the AQP4 pool in distinct membrane domains (8). Immunoblot analyses are not relevant, because the total amount of AQP4 in the neuropil is poorly correlated with the size of the perivascular pool of this protein. Indeed, disruption of the anchoring of the endfoot pool of AQP4 led to a mislocalization, rather than a net loss of AQP4 (3).

Results

On the unaffected side (see *Materials and Methods*), double immunofluorescence analysis showed colocalization of AQP4 with dystrophin (Fig. 1*A*) and α-syntrophin (Fig. 1*C*) around brain microvessels. The same staining pattern was found in the border zone of the ischemic lesion and in ipsilateral cortical areas more distant from the lesion. In the central part of the ischemic neocortex, examined after 24 hr of reperfusion, the perivascular pools of dystrophin (Fig. 1*B*) and α-syntrophin (Fig. 1*D*) largely persisted, whereas the perivascular pool of AQP4 was lost. Only in deep regions of the cortex (and in the striatal core) were vessels found that lacked immunoreactivity for AQP4 as well as dystrophin and α-syntrophin.

Prompted by the results of the immunofluorescence analysis, we used a postembedding immunogold procedure to assess AQP4 expression in the perivascular astrocyte membrane (Figs. 2 and 3). The loss of perivascular AQP4 immunoreactivity in the

Conflict of interest statement: No conflicts declared.

Freely available online through the PNAS open access option.

Abbreviations: AQP4, aquaporin-4; MCAO, middle cerebral artery occlusion.

[††]To whom correspondence may be addressed. E-mail: mahmo@medisin.uio.no, o.p.ottersen@medisin.uio.no, or pagre@cellbio.duke.edu.

© 2006 by The National Academy of Sciences of the USA

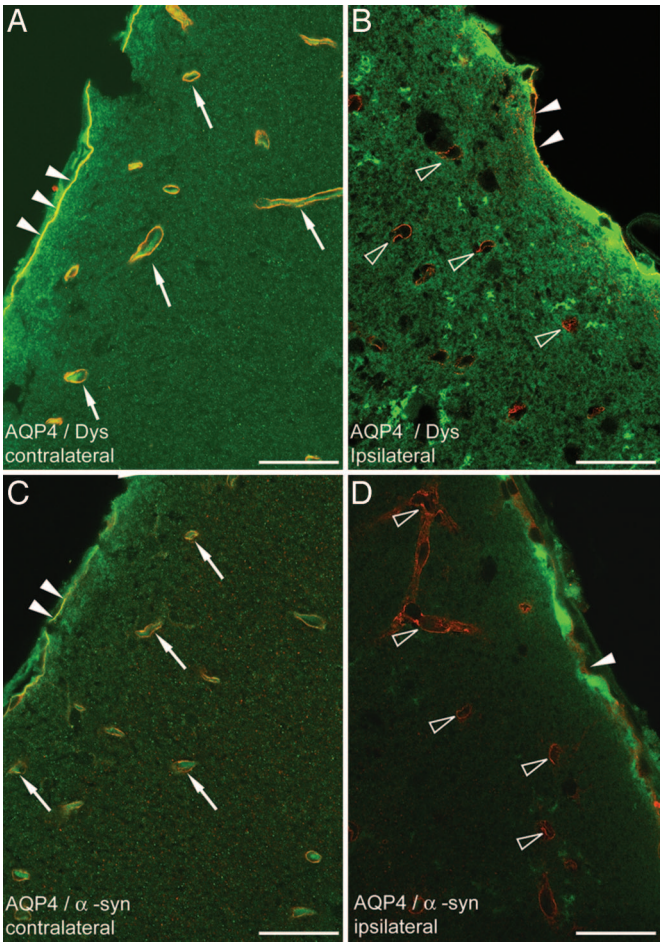

Fig. 1. Immunofluorescence analysis of brains subjected to MCAO (neocortex; 24 hr of reperfusion). (*A* and *C*) Contralateral neocortex, area opposite to ischemic core. (*B* and *D*) Central part of ischemic cortex (Fig. 5, region 4). Yellow labeling surrounding vessels in contralateral cortex indicates colocalization (arrows) of AQP4 (green) and dystrophin (red in *A*) and α-syntrophin (red in *C*). In contrast, vessels in the ischemic cortex are associated with a red signal (open arrowheads), indicating the absence of AQP4 and retention of dystrophin (*B*) and α-syntrophin (*D*). Filled arrowheads indicate the subpial endfeet. Dys, dystrophin; α-syn, α-syntrophin. (Scale bar: 20 μm.)

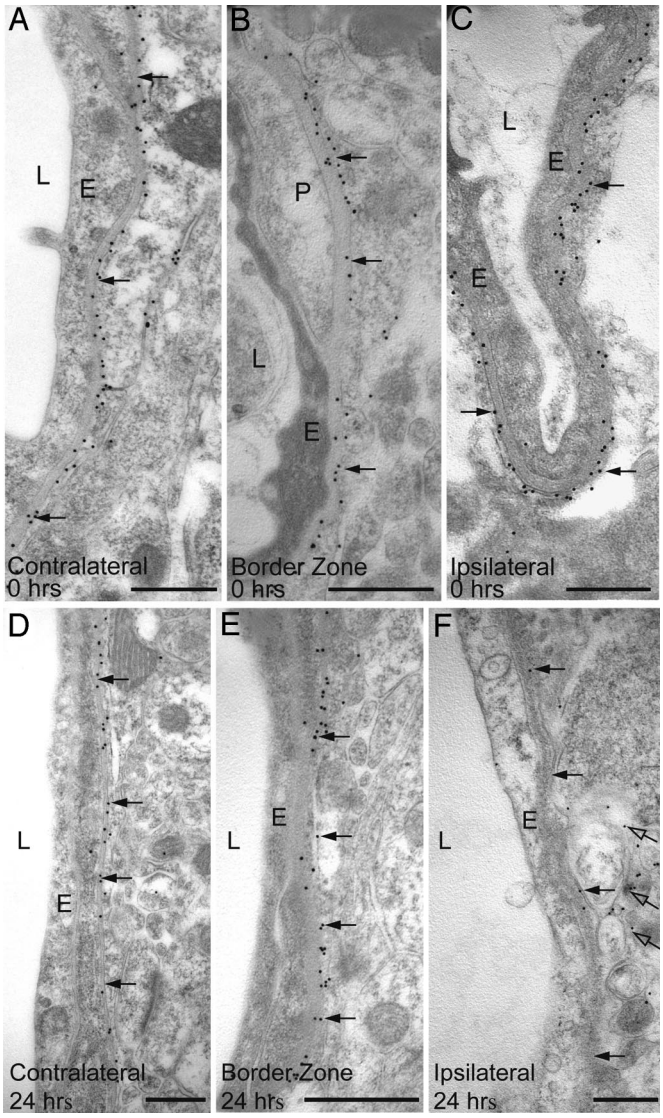

Fig. 2. Immunogold analysis of AQP4 expression immediately (0 hr in *A–C*) and 24 hr (*D–F*) after the onset of reperfusion (0 hr). At 24 hr, there is a pronounced reduction in the number of gold particles (arrows) over perivascular membranes in central part of the ischemic cortex (*F*) compared with the border zone (*E*) and contralateral side (*D*). In the ischemic cortex, AQP4 labeling remains over the abluminal membrane of the perivascular endfeet (open arrows in *F*). E, endothelial cells; L, vessel lumen; P, pericyte. (Scale bar: 0.5 μm.)

neocortical lesion at 24 hr of reperfusion was confirmed (Fig. 2*F*). Visual examination of earlier and later time points (including 0 hr, Fig. 2*C*) revealed no or more modest losses, suggesting that the perivascular AQP4 labeling reached minimum values at ≈24 hr.

The qualitative data were supplemented by a quantitative immunogold analysis of the striatal and neocortical zones of the ischemic lesion (Fig. 3). The contralateral side was used as an internal reference in each animal to minimize the confounding effect of possible differences in fixation efficiency. Each of the four animals analyzed at 24 hr of reperfusion showed a statistically significant loss of perivascular AQP4 in the central part of the ischemic cortex, compared with the corresponding part of the contralateral cortex (Fig. 3). On average, the labeling decreased by 78%, with a minimum of 59% and a maximum of 93%. In contrast, none of the animals displayed any significant loss of AQP4 from perivascular membranes of the cortical border zone. This was true for each group of animals, irrespective of reperfusion time. Indeed, the labeling in the border zone (the intensity of which was slightly depressed at the start of reperfusion) tended to increase toward 24 hr and thence to decrease toward control level (Fig. 3).

Supporting the qualitative analysis, the quantitative data suggested that the pronounced loss of perivascular AQP4 in the central part of the ischemic cortex at 24 hr was not a precipitous event but rather a trough preceded by a gradual decline and followed by a gradual restoration. Thus, at 24, 48, and 72 hr of reperfusion, the loss of AQP4 averaged 78%, 58%, and 45% with significance levels between 0.0058 and 0.0477. At 2 and 6 hr of reperfusion, the immunogold density values for AQP4 were 59% and 80% of control values, respectively, and were not significantly different from these values (*P* values of 0.07 and 0.36, respectively).

The data described above were obtained from the neocortex. We also investigated AQP4 expression in the striatum, which constitutes a major part of the ischemic core. The pattern of changes in the striatum mimicked the pattern of changes in the overlying neocortex, with one notable exception: The tendency

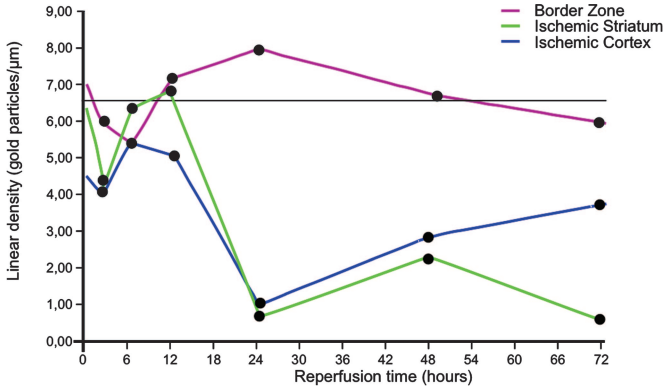

Fig. 3. Time course of AQP4 expression after MCAO. Values along the ordinate represent linear density of gold particles over perivascular membranes (same samples as in Fig. 2). Density values were obtained from the central part of the ischemic cortex (blue), striatal part of the core (green), and cortical border zone (red). The horizontal black line indicates the reference level (calculated from the neocortex and striatum contralateral to the lesion). The values for the ischemic cortex (blue) and striatal core (green) are significantly different from the reference values for reperfusion times of 24, 48, and 72 hr. The corresponding *P* values are 0.0058, 0.0122, and 0.0477 (cortex) and 0.0043, 0.0076, and 0.0052 (striatum), respectively.

toward a recovery of immunolabeling at 72 hr, obvious in the neocortex, was not observed in the striatum (Fig. 3).

In the central part of the ischemic cortex, the abluminal membrane of the endfeet showed scattered gold particles (Fig. 2*F*). This membrane domain is normally almost devoid of gold particles signaling AQP4. The quantitative immunogold analysis of the ischemic cortex revealed no alteration in the α-syntrophin expression level at 0 or 24 hr of reperfusion (data not shown).

Astrocyte endfeet were examined by freeze fracture (Fig. 4*A*). At high magnification, AQP4 square arrays were abundant in the endfoot membrane facing the capillary (Fig. 4*B*), and glial fibrillary acidic protein (GFAP) filaments were abundant in the cytoplasm (faintly detectable at the low magnification in Fig. 4*A*), with either marker providing for positive identification of astrocyte processes. In the border zone (Fig. 4 *C* and *D*), AQP4 square arrays were abundant in membrane P-faces abutting capillaries (Fig. 4*C*), and their imprints were abundant in endfoot membrane E-faces (Fig. 4*D*). The P-faces correspond to the replicated protoplasmic leaflet of split membranes, and the E-faces represent replicated extraplasmic membrane leaflets (9). Endfoot-like processes in the striatal core and overlying neocortex lacked AQP4 square arrays in their plasma membranes (Fig. 4*F*).

Discussion

The present work reveals that the expression level of the perivascular pool of AQP4 undergoes major changes after a transient ischemic insult. These results bear directly on the molecular mechanisms underlying the generation and dissolution of postischemic edema, because the perivascular pool of AQP4 allows bidirectional water flow and hence is likely to be rate-limiting for both water influx and efflux (4).

Our data suggest a biphasic change in perivascular AQP4 expression in the most affected part of the ipsilateral cortex. The initial reduction in AQP4 expression (with minimum values at ≈24 hr) will serve to delimit water influx, whereas the partial recovery of the AQP4 level (from 24 to 72 hr; i.e., subsequent to the culmination of the edema) would be expected to favor absorption of excess fluid. This pattern of changes contrasts with the changes that occur in the cortical border zone. Here, a trend toward an elevated level of AQP4 expression was observed at a

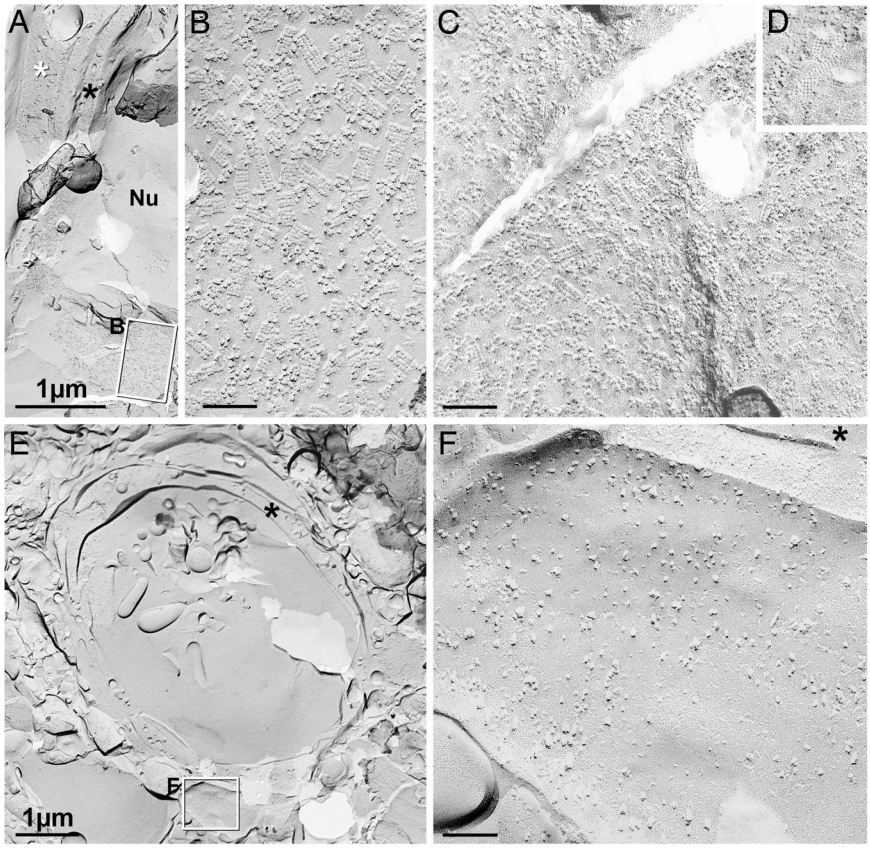

Fig. 4. Conventional freeze fracture images from contralateral cortex (*A* and *B*), cortical border zone (*C* and *D*), and central part of ischemic lesion (*E* and *F*), all from 24 hr of reperfusion after MCAO. (*A*) Low-magnification image from contact region between astrocyte endfoot (white asterisk) and the edge of capillary (black asterisk in cytoplasm). Boxed area encloses P-face of astrocyte, shown at higher magnification in *B*. Nu, endothelial nucleus. (*B*) High-magnification view of P-face of astrocyte endfoot plasma membrane, showing >100 AQP4 arrays in ≈0.3 μm^2. (*C*) P-face of astrocyte endfoot in border zone has AQP4 arrays at approximately the same density as in contralateral control. (*D*) E-face view of AQP4 imprints, also from border zone. (*E*) Low-magnification view of capillary in central part of ischemic lesion. Membrane debris is present in the lumen of the capillary. Boxed area including presumptive astrocyte endfoot shown at higher magnification in *F*. The black asterisk indicates endothelial cytoplasm. (*F*) High-magnification image of E-face of presumptive astrocyte endfoot in central part of ischemic lesion. AQP4 arrays were not detected in this or any other membrane adjacent to capillaries. The black asterisk indicates endothelial cytoplasm. *B–D* and *F* are at the same magnification. (Calibration bars: *A* and *E*, 1 μm; *B*, *C*, and *F*, 0.1 μm.)

time when the AQP4 expression was decreased in the central part of the ischemic cortex.

The present data clearly show that the cortical region most severely affected by the ischemic insult behaves differently from the striatal core when it comes to changes in AQP4 expression in the postischemic phase. Notably, unlike the striatal core, the ischemic cortex shows a partial recovery of perivascular AQP4 toward 72 hr of reperfusion. Taken together with our finding of persistent α-syntrophin and dystrophin labeling, the latter observation suggests that the affected cortex (with the possible exception of the deepest layers) differs from the striatal core by preserving, for 72 hr at least, the integrity of astrocyte membranes after the MCAO insult. On this background we have chosen to distinguish the affected cortex from the striatal core by using the term "central part of the ischemic cortex" rather than the term "cortical core."

The persistence in the cortex of dystrophin and α-syntrophin in the perivascular membrane leaves us with a mechanistic model in which ischemia disrupts the coupling between AQP4 and its anchoring complex. Rapid changes in the size of the perivascular AQP4 pool can be envisaged if the anchoring is severed, because of the high AQP4 concentration gradient between perivascular membranes and other membrane domains (including the abluminal endfoot membrane, which showed increased labeling after ischemia). Our findings are consistent with the idea that an ischemia-induced perturbation of AQP4 anchoring permits a lateral diffusion of AQP4, thereby draining the pool of AQP4 that normally resides in the perivascular membrane. This explanation is in line with previous observations in transfected HEK 293 cells, indicating that truncated AQP4 (lacking the three C-terminal residues that are essential for binding to the dystrophin complex) disappears much more quickly from the membranes than WT AQP4 (3).

Theoretically, the loss of AQP4 immunosignal could be due to conformational changes in AQP4 with a subsequent loss of affinity for the selective antibodies. This possibility could be ruled out by the freeze fracture analysis, which demonstrated a complete loss of the square lattices of particles from the endfoot membranes. Expression studies and analysis of AQP4-null animals have provided conclusive evidence that these square lattices correspond to arrays of AQP4 (10, 11).

We have previously shown by Western blotting that disruption of AQP4 anchoring at the perivascular membrane leads to a mislocalization of AQP4 rather than a net loss (3, 8). Previous studies of the effects of ischemia on AQP4 have not focused on the perivascular (rate-limiting) pool of AQP4 but have analyzed the tissue contents of AQP4 or the level of AQP4 mRNA (12–14). There is evidence of an increased synthesis of AQP4 in the periinfarct zone after MCAO or stroke (14).

The persistence of the perivascular AQP4 pool in the cortical border zone suggests that partial ischemia is not sufficient to interfere significantly with anchoring of AQP4 (although the initial drop in AQP4 expression may be indicative of a transient effect on the anchoring mechanisms). This finding could be exploited diagnostically in attempts to assess the relative volumes of the central part and border zone of the ischemic lesion, given the availability of a ligand that binds selectively to the perivascular pool of AQP4. Our findings are in agreement with a recent study (15) which shows that osmotherapy with 7.5% hyperosmotic saline at 24 hr after MCAO in rats leads to a significant decrease in the brain water content in the cortical border zone (where the perivascular AQP4 expression is retained) but not in the central part of the lesion (where the perivascular AQP4 expression is strongly reduced).

In conclusion, our data suggest that the size of the AQP4 pool that controls the exchange of fluid between brain and blood during edema formation and dissolution is subject to large changes during the reperfusion phase. The magnitude and direction of these changes serve to distinguish the central part from the border zone of the ischemic lesion and must be taken into account in future strategies to develop new therapies targeting AQP4 or associated molecules in the perivascular membrane.

Materials and Methods

Animals. Experimental protocols were approved by the Institutional Animal Care and Use Committee and conform to National Institute of Health guidelines for the care and use of animals. Studies were conducted with male WT C57BL mice allowed ad libitum access to food and drinking water.

Brain Ischemia. Twenty-one mice with body weights of 27–32 g were anesthetized with 1–1.2% halothane in oxygen-enriched air, and rectal temperature was maintained at 37 ± 0.5°C with heating lamps during the entire surgical procedure. Mice were then subjected to MCAO in a randomized fashion as described previously (4). MCAO was verified at 30 min by allowing the animal to awaken and performing neurological deficit scoring as follows: 0, normal motor function; 1, flexion of torso and of contralateral forelimb upon lifting by the tail; 2, circling to the contralateral side but normal posture at rest; 3, leaning to the contralateral side at rest; 4, no spontaneous motor activity. Mice with clear neurological deficits (score of ≥2) were reanesthetized for withdrawal of the suture and reperfusion after 90 min of MCAO. The mice were perfused for immunocytochemistry at different time points after the onset of reperfusion (0, 2, 6, 12, 24, 48, and 72 hr). A few animals were excluded because of subarachnoidal hemorrhage. The final numbers of animals included for electron microscopic analysis were three for 0, 2, 6, 12, and 48 hr of reperfusion; four for 24 hr of reperfusion; and two for 72 hr of reperfusion. Two additional animals were perfused at 24 hr for immunofluorescence analysis. The use of the contralateral side as reference gave statistical significance with a relatively low number of animals (see below).

Tissue was sampled from the striatal core and the overlying neocortex (the "central part of the ischemic cortex"). Samples were also collected from the neocortical border zone (defined as the most peripheral zone of the affected cortex and with less distinct pallor than the core).

Antibodies. Antibodies to AQP4 (polyclonal, Alpha Diagnostics, San Antonio, TX; monoclonal, Serotec, Oxford, U.K.), α-syntrophin [polyclonal (16)], or dystrophin (polyclonal, raised against the C terminus of DP-71; Abcam, Cambridge, U.K.) were used in the present work. The properties of the antibodies have been described (3, 17, 18). The selectivity of the labeling was confirmed by omission of the primary antibody or preadsorption with the immunizing peptide.

Electron Microscopy. Mice were perfused through the heart with 4% formaldehyde in phosphate buffer at pH 6.0, then pH 10.0 (4). For quantitative immunogold studies, tissue blocks were dissected from a 1.0-mm-thick coronal slice through the forebrain. The tissue blocks did not exceed 1 mm in any dimension and were dissected from each of the following five regions (Fig. 5): 1, contralateral neocortex; 2, contralateral striatum; 3, cortical border zone; 4, central part of the ischemic cortex; and 5, striatal core. The tissue blocks were cryoprotected, quick-frozen in liquid propane (−170°C), and subjected to freeze substitution (3, 19). Specimens were embedded in methacrylate resin (Lowicryl HM20; Polysciences, Warrington, PA) and polymerized by UV light below 0°C. Ultrathin sections were incubated with antibodies to AQP4 (polyclonal, 10 μg/ml) or α-syntrophin (1:100) followed by goat anti-rabbit antibody coupled to 15-nm colloidal gold. The sections were examined in a Philips (Eindhoven, The Netherlands) CM10 electron microscope at 60 kV (20, 21).

Fluorescence Microscopy. For immunofluorescence we used 16-μm cryostat sections obtained from brains that had been fixed

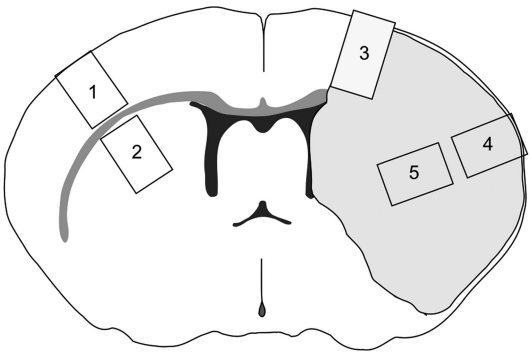

Fig. 5. Diagram of coronal slice through the forebrain. The shaded area on the right side is the area affected by ischemia. Specimens were dissected from the following: 1, contralateral neocortex (control); 2, contralateral striatum (control); 3, cortical border zone; 4, central part of ischemic cortex; and 5, striatal part of the ischemic core.

as described above. The sections were incubated with an antibody to AQP4 (monoclonal, 10 μg/ml) together with anti-dystrophin (5 μg/ml) or anti-syntrophin (1:500) followed by Alexa Fluor 448-conjugated donkey anti-mouse and Cy3-conjugated goat anti-rabbit IgG antibodies and were then viewed and photographed with a Zeiss (Oberkochen, Germany) LSM 5 Pascal confocal microscope (8).

Freeze Fracture. Formaldehyde-fixed tissue blocks from the core region, the border zone, and the contralateral cortex were sectioned at 150 μm, infiltrated with 30% glycerol, frozen by contact with a liquid nitrogen-cooled metal mirror (ULTRA-FREEZE MF7000; RMC Products, Tucson, AZ), fractured and replicated in an RMC/JEOL (JEOL, Tokyo, Japan) 9010c freeze fracture machine, and cleaned with 5.25% sodium hypochlorite bleach (22). Replicas were examined at 100 kV in a JEOL (Peabody, MA) 2000 EX-II transmission electron microscope (TEM). Astrocyte endfeet adjacent to capillaries were photographed stereoscopically at magnifications of $\times$10,000–50,000, with 8° included angle between images. TEM negatives were scanned and digitized by using an ArtixScan 2500f digital scanner (Microtek, Carson, CA) and processed with Adobe Photoshop CS by using minimal (or no) "unsharp mask," maximal contrast expansion with "levels," and selected area "dodging" using brightness/contrast functions to optimize image contrast and definition.

Quantification and Statistical Analysis. For the quantification of AQP4 immunogold labeling, 15–20 digital (16-bit) images from each section (one section per block, giving a total of 1,426 images) were acquired in a blinded manner and quantified with a commercially available image analysis program (analySIS; Soft Imaging Systems, Münster, Germany) (8, 17). Perivascular labeling was measured as gold particles per unit length of astrocyte membrane in direct contact with the pericapillary basal lamina (linear particle density). Particles were included if their centers were localized within 30 nm of the midpoint of the membrane (23). Linear densities of gold particles over astrocyte membranes were determined by an extension of analySIS (Soft Imaging Systems) as described (8, 24). Curves were drawn interactively, and linear densities were determined semiautomatically and transferred to SPSS Version 13 (SPSS, Chicago, IL). Values for individual curve segments were averaged per section (block, animal).

Data were analyzed by a linear mixed model, using the lme function in R (25). Fixed effects were first included for every combination of region and reperfusion time. We assumed a dependency structure with random effects on animals and on regions inside animals. Parameter estimates were obtained by maximum likelihood for the fixed effects and by restricted maximum likelihood for the variances of the random effects. It was found that there were no significant difference in gold particle densities over times for the control regions (contralateral neocortex and striatum; P value of 0.434). Hence, we chose to represent these two regions by a single fixed effect. We assumed a model with variances that differ between regions. For a detailed description see www.med.uio.no/imb/stat/immunogold/index.html.

This work was supported in part by U.S. Public Health Service National Institutes of Health Grant NS 046379 (to A.B.), National Institutes of Health Grants NS 44395 and NS 44010 (to J.E.R.), the Norwegian Research Council, and NordForsk (Nordic Centre of Excellence Program in Molecular Medicine).

1. Nielsen, S., Nagelhus, E. A., Amiry-Moghaddam, M., Bourque, C., Agre, P. & Ottersen, O. P. (1997) *J. Neurosci.* **17,** 171–180.
2. Rash, J. E., Yasumura, T., Hudson, C. S., Agre, P. & Nielsen, S. (1998) *Proc. Natl. Acad. Sci. USA* **95,** 11981–11986.
3. Neely, J. D., Amiry-Moghaddam, M., Ottersen, O. P., Froehner, S. C., Agre, P. & Adams, M. E. (2001) *Proc. Natl. Acad. Sci. USA* **98,** 14108–14113.
4. Amiry-Moghaddam, M., Otsuka, T., Hurn, P. D., Traystman, R. J., Haug, F. M., Froehner, S. C., Adams, M. E., Neely, J. D., Agre, P., Ottersen, O. P., *et al.* (2003) *Proc. Natl. Acad. Sci. USA* **100,** 2106–2111.
5. Vajda, Z., Pedersen, M., Fuchtbauer, E. M., Wertz, K., Stodkilde-Jorgensen, H., Sulyok, E., Doczi, T., Neely, J. D., Agre, P., Frokiaer, J., *et al.* (2002) *Proc. Natl. Acad. Sci. USA* **99,** 13131–13136.
6. Manley, G. T., Fujimura, M., Ma, T., Noshita, N., Filiz, F., Bollen, A. W., Chan, P. & Verkman, A. S. (2000) *Nat. Med.* **6,** 159–163.
7. Papadopoulos, M. C., Manley, G. T., Krishna, S. & Verkman, A. S. (2004) *FASEB J.* **18,** 1291–1293.
8. Amiry-Moghaddam, M., Xue, R., Haug, F. M., Neely, J. D., Bhardwaj, A., Agre, P., Adams, M. E., Froehner, S. C., Mori, S. & Ottersen, O. P. (2004) *FASEB J.* **18,** 542–544.
9. Branton, D., Bullivant, S., Gilula, N. B., Karnovsky, M. J., Moor, H., Muhlethaler, K., Northcote, D. H., Packer, L., Satir, B., Satir, P., *et al.* (1975) *Science* **190,** 54–56.
10. Furman, C. S., Gorelick-Feldman, D. A., Davidson, K. G., Yasumura, T., Neely, J. D., Agre, P. & Rash, J. E. (2003) *Proc. Natl. Acad. Sci. USA* **100,** 13609–13614.
11. Verbavatz, J. M., Ma, T., Gobin, R. & Verkman, A. S. (1997) *J. Cell Sci.* **110,** 2855–2860.
12. Lu, H. & Sun, S. Q. (2003) *Chin. Med. J. (Engl. Ed.)* **116,** 1063–1069.
13. Meng, S., Qiao, M., Lin, L., Del Bigio, M. R., Tomanek, B. & Tuor, U. I. (2004) *Eur. J. Neurosci.* **19,** 2261–2269.
14. Taniguchi, M., Yamashita, T., Kumura, E., Tamatani, M., Kobayashi, A., Yokawa, T., Maruno, M., Kato, A., Ohnishi, T., Kohmura, E., *et al.* (2000) *Brain Res. Mol. Brain Res.* **78,** 131–137.
15. Chen, C. H., Toung, T. J., Sapirstein, A. & Bhardwaj, A. (2006) *J. Cereb. Blood Flow Metab.* **26,** 951–958.
16. Peters, M. F., Adams, M. E. & Froehner, S. C. (1997) *J. Cell Biol.* **138,** 81–93.
17. Amiry-Moghaddam, M., Williamson, A., Palomba, M., Eid, T., de Lanerolle, N. C., Nagelhus, E. A., Adams, M. E., Froehner, S. C., Agre, P. & Ottersen, O. P. (2003) *Proc. Natl. Acad. Sci. USA* **100,** 13615–13620.
18. Amiry-Moghaddam, M., Frydenlund, D. S. & Ottersen, O. P. (2004) *Neuroscience* **129,** 999–1010.
19. Takumi, Y., Ramirez-Leon, V., Laake, P., Rinvik, E. & Ottersen, O. P. (1999) *Nat. Neurosci.* **2,** 618–624.
20. Amiry-Moghaddam, M., Lindland, H., Zelenin, S., Roberg, B. A., Gundersen, B. B., Petersen, P., Rinvik, E., Torgner, I. A. & Ottersen, O. P. (2005) *FASEB J.* **19,** 1459–1467.
21. Puwarawuttipanit, W., Bragg, A. D., Frydenlund, D. S., Mylonakou, M. N., Nagelhus, E. A., Peters, M. F., Kotchabhakdi, N., Adams, M. E., Froehner, S. C., Haug, F. M., *et al.* (2006) *Neuroscience* **137,** 165–175.
22. Rash, J. E. & Yasumura, T. (1992) *Microsc. Res. Tech.* **20,** 187–204.
23. Matsubara, A., Laake, J. H., Davanger, S., Usami, S. & Ottersen, O. P. (1996) *J. Neurosci.* **16,** 4457–4467.
24. Mathiisen, T. M., Nagelhus, E. A., Jouleh, B., Torp, R., Frydenlund, D. S., Mylonakou, M.-N., Amiry-Moghaddam, M., Covolan, L., Utvik, J. K., Riber, B., *et al.* (2006) in *Neuroanatomical Tract-Tracing 3: Molecules, Neurons, and Systems*, eds. Zaborszky, L., Wouterlood, F. G. & Lanciego, J. L. (Springer, New York), pp. 72–108.
25. Pinheiro, J. C. & Bates, D. M. (2002) *Mixed Effects Models in S and S-PLUS* (Springer, New York).